# Optimal Shape Design of Rotor Slot in Squirrel-Cage Induction Motor Considering Torque Characteristics

Gyeorye Lee, Seungjae Min, and Jung-Pyo Hong

Department of Automotive Engineering, Hanyang University, Seoul, 133-791, Korea

**Induction motors are widely used in various industrial applications with different torque-speed characteristics. Since the configuration of the rotor slot has a great impact on the electromagnetic torque-speed characteristics, a design optimization process is necessary to improve the motor performance of the induction motor. The material boundaries of the rotor slot are represented by a level set function, and a voltage driven time-harmonic field analysis is performed to estimate the characteristics of the induction motor. An optimization problem is formulated to maximize the torque at one speed either a rated or starting condition constrained by the torque at other speeds, starting currents and efficiency. A level set equation with an augmented Lagrangian method is derived to find the optimal design. Optimal results are achieved by updating the sequential changes of the material region driven by the shape derivative. The design flexibility of the proposed method is confirmed to obtain National Electrical Manufacturers Association (NEMA) designs satisfying different torque characteristics.**

***Index Terms*—Induction motor, level set method, optimal design, rotor slot, torque-speed characteristics.**

## I. Introduction

INDUCTION motors are widely used in various industrial applications due to their simplicity, robustness and low cost. Because the torque-speed characteristics of induction motors vary for many applications, the National Electrical Manufacturers Association (NEMA) classified motor characteristics mainly into four designs and explained their applications [1]. The torque-speed characteristics are critically affected by the shape of the rotor slot, thus studies on the geometry of the rotor slot to improve motor performance have been performed. The rotor slot design process traditionally results in shapes that are not radically different from existing designs and thus depend upon the designer's intuition from work experience of many years. However, many studies, including shape optimization, have been carried out to improve the performance of induction motors. The optimization of the geometry of closed rotor slots to obtain maximum efficiency was proposed using a deterministic optimization method [2]. Stochastic methods, such as genetic algorithms, were applied to find the global minimum [3] and identify multiple optima [4]. However, the desired improvements in motor performance are elusive using these methods, as the set of *a priori* known design parameters and dimensions are controlled. To overcome this limitation, the topology optimization, which finds optimal material distributions within a given design domain subject to certain criteria, has been applied to the design of induction motors [5]. Conventional element-based topology optimization methods suffer from mesh-dependent boundaries for motor design problems. Recently, level set based design optimization has been successfully applied for the stator design of the permanent magnet motor to determine the optimal distribution of nonlinear ferromagnetic material [6]. This can naturally avoid numerical problems in boundary expressions and represent the geometric boundaries precisely.

Manuscript received November 10, 2012; revised December 31, 2012; accepted December 31, 2012. Date of current version May 07, 2013. Corresponding author: S. Min (e-mail: seungjae@hanyang.ac.kr).

Color versions of one or more of the figures in this paper are available online at http://ieeexplore.ieee.org.

Digital Object Identifier 10.1109/TMAG.2013.2239626

The rotor design of an induction motor is critical to satisfy the performance specification because the torque speed profile is largely determined by the rotor configuration. One important focus is on the shape of the rotor slot, as it is one of the most important factors in improving the performance of induction motors [7], [8].

In this paper, the level set function is employed to represent the material boundaries between the rotor slot material and the nonlinear ferromagnetic material in the rotor. Additionally, the relative permeability property of the material is determined by the level set distribution. The optimization problems are formulated to maximize the rated torque under the starting torque constraint or maximize the starting torque under the rated torque constraint. In addition, the starting current, efficiency and material usage can be specified as constraints. To deal with the objective functions and multiple constraints, an augmented Lagrangian method [9] was applied. For the time-harmonic magnetic field analysis, a voltage driven analysis was performed due to the changed shape during the optimization process. The implicit material boundaries were moved by the speed function, which governs the level set equation and normal velocity calculated using the sensitivities of the objective function, as well as the constraint via the adjoint variable method.

## II. Problem Formulation

### A. Shape Representation in the Magnetic Field

The level set function ($\phi(\mathbf{x})$) [6], defined non-parametrically as a set of real-valued functions, is introduced to represent the boundary between the rotor slot domain and the core domain, where $\mathbf{x}$ stands for an arbitrary position in the design domain. Using the level set function, an arbitrary shape for the rotor of an induction motor composed of aluminum (Al) and ferromagnetic material (FM) can be implicitly represented through an interpolation scheme based on the magnetic permeability. By assuming that the level set function is also implicitly a function of the fictitious time $t$, as time $t$ is advanced, the boundary is updated as an evolving boundary process that would reach an optimal configuration.

To represent the distribution of aluminum and nonlinear ferromagnetic material in the rotor, the magnetic permeability $(\mu)$, varied by the level of the magnetic flux density $(\mathbf{B})$ and electric conductivity $(\sigma)$, are employed as the constitutive parameter and can be defined using a level set function as

$$\sigma(\phi) = \sigma_{Al} H(\phi) + \sigma_{\rm FM}(1 - H(\phi))$$
$$\mu(\phi, \mathbf{B}) = \mu_{Al} H(\phi) + \mu_{\rm FM}(\mathbf{B})(1 - H(\phi)) \qquad (1)$$

where $\sigma_{Al}$ and $\sigma_{\rm FM}$ are the electric conductivity, $\mu_{Al}$ and $\mu_{\rm FM}$ are the magnetic permeabilities of the aluminum and ferromagnetic material respectively, and $H(\phi)$ is the smooth Heaviside function where it is continuous near the boundary, to avoid numerical instability.

### B. Performance Calculation

Since this study considers steady state conditions with sinusoidal supply, a time-harmonic approach has been used to perform the machine simulations. The governing equation of the two-dimensional electromagnetic field computation model with electrical angular speed $\omega$ and rotor slip $s$ is written as follows:

$$\nabla \times \left(\frac{1}{\mu}\nabla \times \mathbf{A}\right) = \mathbf{J}_s - js\omega\sigma\mathbf{A} \qquad (2)$$

where $\mathbf{A}$ is the magnetic vector potential and parallel to $\mathbf{J}_s$, the current density in the stator slots.

To consider the change of the electromagnetic parameters caused by the shape change of the level set function, a voltage driven finite element analysis is performed. The voltage equation is formulated as

$$V = R_m I_s + j\omega L_m I_s + E_m \qquad (3)$$

where $R_m$ is the total resistance of the motor, $L_m$ is the leakage inductance of the end coil and $E_m$ is the back EMF of the motor. As the shape of the rotor slot changes during the optimization process, an updated induced current is estimated by the voltage equation.

### C. Design Optimization

The level set function to represent the rotor slot is the design variable where the boundaries between the ferromagnetic material (rotor) and aluminum (rotor slot) evolve. In order to improve the motor performance, an objective function is proposed to maximize the rated or starting torque $(T_{\rm rated/starting})$ in the air-gap at a specific rated rotor slip depending on the torque characteristics. Based on the magnetic field distribution, the electromagnetic torque was calculated using Maxwell's stress-tensor method [10]. The first constraint is the starting or rated torque $(T_{\rm starting/rated})$ which is not taken as the objective function. Since an excessive starting current affects performance, the second constraint restrains it by the maximum allowable current value. The volume fraction (VF), ratio of the material used and the volume of the design domain $(\Omega)$ of the rotor slot is specified as the third constraint. Lastly, the efficiency is included in constraints to guarantee the minimum design requirement. The output power $(P_{\rm out})$ and the power loss $(P_{\rm loss})$ are considered in the evaluation of the efficiency and the power loss consists of the copper loss and the core loss [11]. Therefore, the design optimization problem to maximize the torque using the level set method can be formulated as

$$\begin{aligned}
&\text{Find}\{\mathbf{x}(t) \mid \phi(\mathbf{x}(t), t) = 0\} \text{ to} \\
&\text{maximize} \quad f = T_{\rm rated/starting} \\
&\text{subject to} \quad g_1 = T_{\rm starting/rated} \geq T^*, \\
&\qquad g_2 = I_{\rm starting} \leq I^*, \\
&\qquad g_3 = \mathrm{VF} \leq \mathrm{VF}^*, \\
&\qquad g_4 = \frac{P_{\rm out}}{P_{\rm out} + P_{\rm loss}} \times 100 \geq \eta^*. \qquad (4)
\end{aligned}$$

The evolution of the boundary $(\phi(\mathbf{x}) = 0)$ is obtained by differentiating with respect to time and yields, the following Hamilton-Jacobi convection equation. The optimization problem is solved by providing the appropriate velocity function values of $V_n$ and the optimal configuration can be obtained when the optimality conditions are satisfied as

$$\begin{aligned}
\frac{\partial \phi(\mathbf{x})}{\partial t} &= V_n |\nabla\phi| \\
&= \left\{\frac{df}{d\phi} + \sum_{i=1}^{n}(\lambda_i + p_i g_i)\frac{dg_i}{d\phi}\right\}|\nabla\phi| = 0 \qquad (5)
\end{aligned}$$

where the Lagrange multiplier $\lambda_i$ is determined by the active constraint condition.

$$\lambda_{i,k+1} = \max(\lambda_{i,k} + p_i g_{i,k}, 0) \qquad (6)$$

More accurate numerical results can be obtained by initializing the level set function as the signed distance function $(|\nabla\phi| = 1)$.

The flowchart in Fig. 1 illustrates the overall procedure of the proposed method. The level set function is initialized as a signed distance function. Next, the equilibrium equations of the time-harmonic field are solved to compute the magnetic potential using the finite element method at a specific rotor slip where the objective function $f(\phi(\mathbf{x}))$ is then calculated. Thereafter, the evaluation of the sensitivities of the objective function and the constraints with respect to $\phi$ is performed to compute the normal velocity. Finally, the level set function is updated based on the level set equation.

## III. Design Example

The proposed method is applied to the optimal shape design of the rotor slot in a three-phase induction motor [12] with 20 aluminum cast slots at their rated load, the fixed rotor slip value of 0.034 as shown in Fig. 2. The air-gap is 0.5 mm thick and the stator has a distributed double-layer winding with 208 turns per phase. The stator and rotor magnetic cores made of laminations are nonlinear, with a saturation flux density of 2.1 T. The dimensions and specifications of the induction motor are summarized in Table I. The boundary conditions consist of zero magnetic flux on the outer surface of the stator and the inner surface of the rotor and the periodicity on both sides of the design domain. The reference design involves the time-harmonic

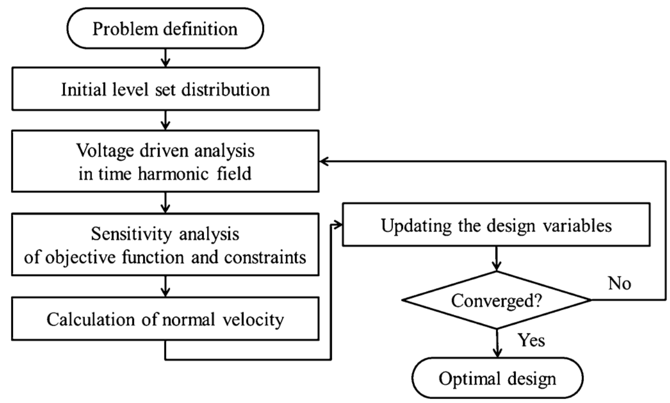


Fig. 1. Optimization process.

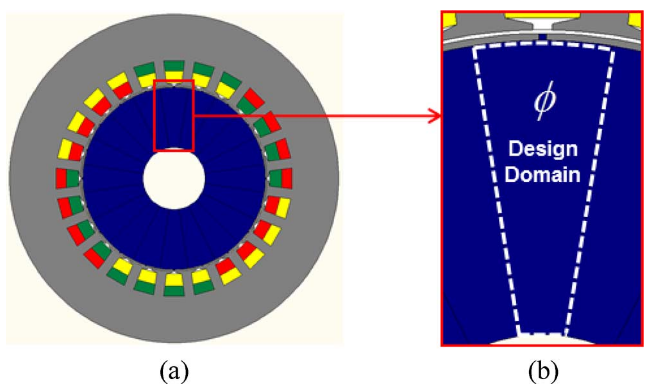


Fig. 2. Induction motor: (a) reference design; (b) design domain.

TABLE I
DIMENSIONS AND SPECIFICATIONS OF INDUCTION MOTOR TEST CASE

| Item | Value | Unit |
|---|---|---|
| Rated power | 7.5 | kW |
| Rated voltage | 380 | $V_{rms}$ |
| Efficiency | 86.5 | % |
| Source frequency | 50 | Hz |
| Pole number | 2 | |
| Stator/rotor slot number | 24/20 | |
| Stator/rotor outer diameter | 212/119 | mm |
| Stack length | 125 | mm |

nonlinear operation of a double cage induction motor, and the end ring resistance is considered in calculating the rotor slot resistance. A voltage driven analysis is performed to consider the variation of the electric parameters including the current with respect to the shape change. For optimal design, the efficiency of the reference design must be secured so that the minimum value of efficiency $(\eta^*)$ is set to 86.5% throughout the example.

### *A. Design for NEMA Design C*

Since the reference design corresponds with the NEMA Design C, the optimization problem is formulated to maximize the starting torque subject to the minimum rated torque and the maximum induced current as shown in Table II. Fig. 3 shows the configuration comparison of the rotor slot between the reference

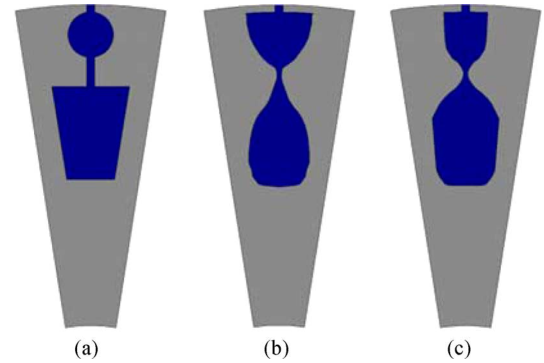


Fig. 3. Optimal design of rotor slot (a) reference model; (b) design C without VF; (c) design C with VF.

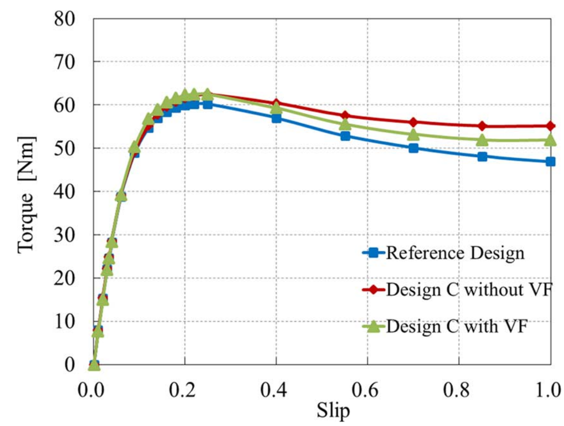


Fig. 4. Torque-slip characteristics of example A.

TABLE II
PROBLEM FORMULATIONS FOR NEMA DESIGNS

| Item \ Design | A | B | C without VF | C with VF | D |
|---|---|---|---|---|---|
| $T(f)$ | rated | rated | starting | starting | starting |
| $T^*(g_1)$ | 42 (starting) | 42 (starting) | 24.6 (rated) | 24.6 (rated) | 25.3 (rated) |
| $I^*(g_2)$ | N/A | 60 | 51.2 | 51.2 | N/A |
| $VF^*(g_3)$ | N/A | N/A | N/A | 0.245 | N/A |

design (a) and the optimal designs when VF is not constrained (b) and the same amount of material in the reference design is specified (c). It should be noted that both the optimal configurations are converged to the double cage with an hourglass-like shape and the straight line at the top is identified to optimize the torque. The case without VF generates a larger area of rotor slot by 3.3% compared to the others and the case with VF has a different shape at the top and bottom portions compared to the reference model. The corresponding torque-slip profiles are drawn in Fig. 4, and the case without VF outperforms the other designs. The data of optimized performance are summarized in Table III.

### *B. Design for Other NEMA Designs*

The optimal shape design of the rotor slot by controlling the objective torque and the constraint limits enables the reference

TABLE III
PERFORMANCE COMPARISON

| Item \ Design | A | B | C without VF | C with VF | D |
|---|---|---|---|---|---|
| $T_{rated}[Nm]$ | 37.84 | 31.39 | 24.60 | 24.60 | 25.47 |
| $T_{starting}[Nm]$ | 46.80 | 42.78 | 55.21 | 52.00 | 81.39 |
| $I_{starting}[A_{rms}]$ | 71.40 | 59.00 | 51.18 | 51.16 | 56.59 |
| VF | 0.366 | 0.318 | 0.253 | 0.245 | 0.119 |
| Efficiency[%] | 86.9 | 86.5 | 86.5 | 86.5 | 87.7 |

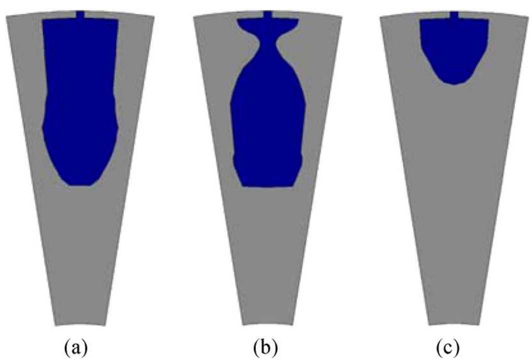


Fig. 5. Optimal design of rotor slot (a) design A; (b) design B; (c) design D.

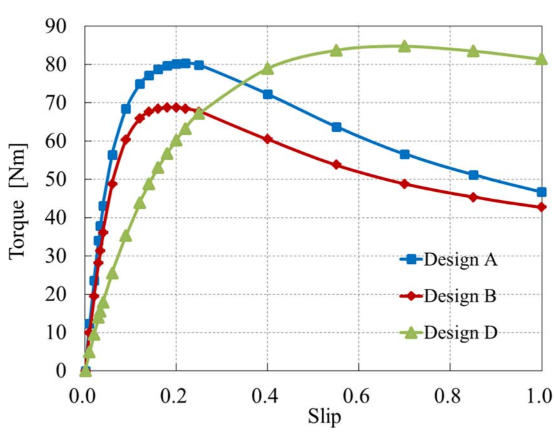


Fig. 6. Torque-slip characteristics of example B.

design to provide different operating characteristics. The rated torque is maximized under the minimum starting torque constraint to simulate NEMA Design A and B, and vice versa for NEMA Design D. The maximum induced current constraint is applied to the NEMA Design B only. The specific data for the optimization problem formulation are listed in Table II.

Fig. 5 shows the optimal shape of the rotor slot in each NEMA design case. Since no VF is restrained, the material boundary is moved to optimize the target torque within a feasible region constructed by constraints. It is noted in Fig. 6 that the corresponding torque-slip profile has good agreement with the typical operating characteristics. It is found in Table III that performance satisfies the constraints.

## IV. CONCLUSION

The optimal configuration design of the rotor slot to consider the operating characteristics is achieved by using a level set based design optimization incorporated with time-harmonic magnetic field analysis. A new optimization problem formulation is proposed for the universal design of an induction motor and the target torque is maximized while all the constraints are satisfied. It is confirmed that the optimal shape design of the rotor slot has a substantial effect on the torque-slip characteristics of the induction motor. The NEMA design examples demonstrate outstanding flexibility in handling geometric changes of the rotor slot with different torque-slip characteristics.

## ACKNOWLEDGMENT

This work was supported by Basic Science Research Program through the National Research Foundation of Korea (NRF) funded by the Ministry of Education, Science and Technology (2012R1A1B3002741) and the MKE (The Ministry of Knowledge Economy), Korea, under the CITRC (Convergence Information Technology Research Center) support program (NIPA-2012-H0401-12-2003) supervised by the NIPA (National IT Industry Promotion Agency).

## REFERENCES

[1] *NEMA Energy Management Guide for Selection and Use of Fixed Frequency Medium AC Squirrel-Cage Polyphase Induction Motors*, NEMA Standards Publication, MG 10-2001(R2007), National Electrical Manufacturers Association, 2007.

[2] S. Williamson and C. I. McClay, "Optimization of the geometry of closed rotor slots for cage induction motors," *IEEE Trans. Indust. Appl.*, vol. 32, no. 2, pp. 560–568, 1996.

[3] D.-H. Cho, H.-K. Jung, and C.-G. Lee, "Induction motor design for electric vehicle using a niching genetic algorithm," *IEEE Trans. Indust. Appl.*, vol. 37, no. 4, pp. 994–999, 2001.

[4] M. Cunkas and R. Akkaya, "Design optimization of induction motor by genetic algorithm and comparison with existing motor," *Mathemat. Comput. Appl.*, vol. 11, no. 3, pp. 193–203, 2006.

[5] S.-M. Wang, J.-N. Kang, and J.-C. Noh, "Topology optimization of a single-phase induction motor for rotary compressor," *IEEE Trans. Magn.*, vol. 40, no. 3, pp. 1591–1596, 2004.

[6] J. Kwack, S. Min, and J.-P. Hong, "Optimal stator design of interior permanent magnet motor to reduce torque ripple using the level set method," *IEEE Trans. Magn.*, vol. 46, no. 6, pp. 2108–2111, 2010.

[7] V. Fireteanu, T. Tudorache, and O. A. Turcanu, "Optimal design of rotor slot geometry of squirrel-cage type induction motors," in *Proc. IEMDC*, 2007, pp. 537–542.

[8] D. Zhang, C.-S. Park, and C.-S. Koh, "A new optimal design method of rotor slot for three-phase squirrel cage induction motor for NEMA class D speed-torque characteristic using multi-objective optimization algorithm," *IEEE Trans. Magn.*, vol. 48, no. 2, pp. 879–882, 2012.

[9] S. Yamasaki, T. Nomura, A. Kawamoto, K. Sato, K. Izui, and S. Nishiwaki, "A level set based topology optimization method using the discretized signed distance function as the design variables," *Structural Multidisciplinary Optim.*, vol. 41, no. 5, pp. 685–698, 2009.

[10] N. Sadowski, Y. Lefevre, M. Lajoie, and J. M. Cros, "Finite element torque calculation in electrical machines while considering the movement," *IEEE Trans. Magn.*, vol. 28, no. 2, pp. 1410–1413, 1992.

[11] K. Yamazaki and Y. Haruishi, "Stary load loss analysis of induction motor-comparison of measurement due to IEEE standard 112 and direct calculation by finite-element method," *IEEE Trans. Indust. Appl.*, vol. 40, no. 2, pp. 543–549, 2004.

[12] R. Escarela-Perez, E. Melgoza, and J. Alvarez-Ramirez, "Coupling circuit systems and finite element models: A 2-D time-harmonic modified nodal analysis framework," *IEEE Trans. Magn.*, vol. 45, no. 2, pp. 707–715, 2009.